Monitoring of Precipitable Water Vapor and Cloud Liquid Path from Scanning Microwave Radiometers During the 2003 Cloudiness Inter-Comparison Experiment

V. Mattioli
Department of Electronic and Information Engineering
University of Perugia
Perugia, Italy

E. R. Westwater
Cooperative Institute for Research in Environmental Sciences
University of Colorado
National Oceanic and Atmospheric Administration
Environmental Technology Laboratory
Boulder, Colorado

V. Morris
Pacific Northwest National Laboratory
Richland, Washington

Introduction

Ground-based microwave radiometers (MWR) are widely used to measure atmospheric precipitable water vapor (PWV) and cloud liquid path (CLP). Comparisons of PWV derived from MWRs with water vapor retrievals from instruments like radiosondes, Global Positioning System (GPS) and Raman lidar are described in (Westwater 1993, Rocken et al. 1995, Basili et al. 2001, Han et al. 1994), but estimates of CLP are less characterized at present, since cloud liquid is not directly measured by RAOBs. Comparisons with aircraft in situ measurements have been made (Westwater et al. 2001), but further investigations are needed. This work is intended to explore the scanning capability of ground-based MWRs. MWR measurements were analyzed to retrieve the spatial distributions of PWV and CLP in the atmosphere, with the aim of improving the accuracy of parameterizations describing processes involved in the formation and evolution of clouds. Three dual-channel scanning MWRs at 23.8 and 31.4 GHz were continuously operated for two months (March and April 2003) during the Cloudiness Inter-Comparison Experiment (CIC) intensive operating period (IOP). The IOP was conducted at the Atmospheric Radiation Measurement (ARM) Program's Southern Great Plains (SGP) site in north-central Oklahoma. Data from the three MWRs were compared during clear-sky condition to assess their agreement. Differences of the order of 0.3 K root mean square (rms) were obtained. Clear conditions were determined by using lidar measurements.

Two different tipping calibration algorithms were applied, the Environmental Technology Laboratory (ETL) calibration method (Han and Westwater 2000) and the ARM calibration algorithm (Liljegren

2000) during clear and cloudy conditions. We evaluated the two calibration methods on the brightness temperature measurements as well as on PWV and CLP retrievals. Brightness temperatures and PWV were also compared with radiosonde observation (RAOB) computations. The RAOBs contained the Vaisala RS90 humidity sensor, and were launched at least four times a day at the same site. PWV and CLP retrievals at each angle in presence of clouds were analyzed. We also compared the observed structures with optical and infrared cloud images, as well as ARM operational cloud boundary products.

Instrument Deployment and Observation Strategies

The SGP central facility site in north-central Oklahoma is a field measurement site operated by U.S. Department of Energy's ARM Program, and consists of in situ and remote-sensing instruments arranged over approximately 143,000 square kilometers. The presence of such arrays of instruments offers an effective opportunity for testing and improving the performance of cloud and radiative models and parameterizations. The operational SGP central facility MWR C1 scans continuously at five angles (19.35, 23.4, 30.15, 41.85, 90.0 degrees) in east-west direction during clear conditions, but shifts to the zenith viewing line-of-site (LOS) mode during cloudy conditions. The half power beamwidth of the two channels at 23.8 and 31.4 GHz is 5.9 and 4.5 degrees respectively.

Two other MWRs of same type, E14 and S01, supplemented the operational MWR for 2 months during the CIC-IOP at the SGP site. The first scanned continuously (i.e., not shifting to the LOS mode during cloudy conditions) in the same vertical plane as that of operational unit, while S01 was scanning continuously in north-south direction, orthogonal to the other two.

Retrieval Method Description

Brightness temperatures measured at 23.8 GHz and at 31.4 GHz allow water vapor and liquid water retrieval along a given direction. Atmospheric water vapor observations are made at 23.8 frequency, near the "hinge point" of the water vapor emission line, while cloud liquid, emitting in a continuum that increases with frequency, prevails in the 31.4 GHz measurement. Sky equivalent brightness temperatures T_B measured by the radiometer are provided by Eq. 1 (Han and Westwater 2000, Liljegren 2000):

$$T_B = T_{ref} + \Gamma(V_{sky}-V_{ref}) \tag{1}$$

where T_{ref} (K) is the reference target temperature, V_{sky} and V_{ref} (counts) are the output signal when the radiometer is looking at the sky and at the reference target respectively. Γ (K/counts) is a multiplicative factor described in Eq. 2:

$$\Gamma = f_w T_{nd}/(V_{ref+nd} - V_{ref}) = f_w G \tag{2}$$

where f_w is the polycarbonate foam window loss factor, T_{nd} is the noise diode injection temperature and V_{ref+nd} the signal when the radiometer is looking at the reference target and the signal from the noise diode is injected. G is the radiometer gain.

Under the assumption of non-scattering atmosphere in local thermodynamic equilibrium, the T_B observed at a direction **r**, for each frequency f, is given by Eq. 3:

$$T_B(r,f) = T_C \, e^{-\tau_f(0,r)} + \int_0^\infty T(r')\alpha(f,r')e^{-\tau_f(r',r)}dr' \tag{3}$$

where T_C is the cosmic background emission, (2.75 K); T(z) is the physical air temperature (K); **r** is the vector position of the emitting air volume (km), $\alpha(f,r)$ is the atmospheric absorption coefficient (Np km^{-1}), $\tau f(0,r)$ is the atmospheric opacity and $\tau_f(r',r)$ is the optical depth. Being not a linear function of PWV and CLP, it is convenient to convert T_B into the atmospheric opacities τ_f (Westwater 1993) as in Eq. 4, by using the mean radiating temperature $T_{mr}(f)$ (Westwater 1993).

$$\tau_f = \ln[(T_{mr}(f)-T_C)/(T_{mr}(f)-T_B(f))] \tag{4}$$

Neglecting scattering and ice contributions water vapor and liquid water can, therefore, be estimated as shown in Eqs. 5-6:

$$PWV = a_0 + a_1\tau_{23} + a_2\tau_{31} \tag{5}$$

$$CLP = b_0 + b_1\tau_{23} + b_2\tau_{31} \tag{6}$$

Retrieval coefficients a_i and b_i were estimated by linear regression for each month on the basis of 10 years of RAOB data launched at the SGP.

Radiometer Calibration Algorithms

In our work we examined two calibration techniques, the ETL tipping calibration method (Han and Westwater 2000), and the ARM automatic self-calibration (Liljegren 2000). The first algorithm is based on measurements of opacity as a function of air mass, defined as the ratio of the opacity at a direction θ and the opacity at zenith, to derive for each tip curve the gain correction f_wT_{nd} in Eq. (2), under the assumption of stratified atmosphere. ARM MWRs elevation angles are close to air mass 3, 2.5, 2, 1.5, and 1. Angles on both sides of zenith are used to assure horizontal homogeneity. In ARM calibration outputs of many tip-curves (>500) that satisfy the homogeneity condition during clear-sky are considered to extract a linear relationship between the noise diode injection temperature T_{nd} and the temperature of the blackbody target T_{ref}.

Data Analysis

We first compared T_Bs at 23.8 and 31.4 GHz measured at zenith by the three radiometers for the period of CIC IOP in clear-sky conditions, matching the measurements with a ten minutes average. Clear and cloudy conditions were identified by using ARM product from the Vaisala CT25K ceilometer.

Table 1 summarizes the comparisons of E14 and S01 respect to C1, T_Bs being calibrated with ETL algorithm. Slope and intercept of the regression line were computed to be consistent with

C1 measurements, and the standard error (Se) of estimation after the regression is also reported. Agreement of the order of 0.3-0.4 K rms between the radiometers is evident from the table, showing that the radiometers are well calibrated. The estimated accuracy of MWR calibration is of the order of 0.2-0.3 K rms (Liljegren 2000).

Table 1. MWR Comparison. Sample size is 2784 for clear-sky. Bias and standard deviation are referred to T_B (C1) -T_B (MWRs).

	Bias [K]	**Std [K]**	**slope**	**int. [K]**	**Se [K]**
S01 23 GHz	-0.24	0.30	0.985	0.063	0.161
E14 23 GHZ	0.18	0.30	1.005	0.102	0.137
S01 31 GHZ	-0.15	0.13	1.017	-0.376	0.089
E14 31 GHz	0.27	0.13	1.002	-0.260	0.069

Comparisons with ROABs

Table 2 shows the comparison of the brightness temperatures from MWR C1 respect to RAOBs. T_{BS} were computed using a microwave radiative transfer model (Schroeder and Westwater 1993) applying the absorption coefficients algorithm developed by Rosenkranz (1998). RAOBs were deployed with the Vaisala RS90 humidity sensor, and were available four times a day at SGP site. Similar values of bias and standard deviation were found for the three radiometers after adjustment. Comparisons applying ETL and ARM calibration methods to the radiometers data have been made, and are presented in the table.

Table 2. MWR C1 Brightness Temperatures Compared with RAOBs Applying ETL and ARM Calibration Algorithm. Sample size is 89. Bias and standard deviation are referred to T_B(MWR)-T_B(RAOBs). Absorption model is Rosenkranz (1998).

	Freq.	**Bias [K]**	**Std. [K]**
ETL Calibration	23 GHz	0.29	0.80
	31 GHz	0.03	0.34
ARM Calibration	23 GHz	0.57	0.78
	31 GHz	0.14	0.33

Table 3 shows PWV computed from MWR E14 compared to PWV from RAOB's. For this analysis, our dataset was also partitioned in clear and cloudy condition.

When we examined retrievals from both calibrations, as can be noted also from the summary of Table 2 and Table 3, we found that ETL calibration produces smaller variance during clear conditions but ARM calibration is more stable during period of extended clouds. MWRs versus RAOB comparisons seem also to show that the new Vaisala humidity sensor is not presenting the dry bias problem (Wang et al. 2002) as shown previously (Cimini et al. 2002a, 2002b, 2003).

Table 3. Comparison of rms Difference Between PWV from MWR E14 and from RAOBs. ARM and ETL calibration methods are used. The PWV retrieval algorithm is based on Rosenkranz (1998). Sample sizes are 120 for clear-sky, 39 for cloudy conditions, and 191 when we considered the entire dataset. We also found a disagreement 32 times between RAOB's and the lidar in evaluating clear-sky condition. In particular we found 2 episodes of cloud shown by RAOB's that were not detected by the ceilometer, 12 episodes of no cloud indicated by RAOB when the ceilometer was indicating clouds, and the remaining episodes are classified as "uncertain" from the ceilometer.

	PWV rms [cm]		
	Clear-Sky	**Cloudy**	**Entire Dataset**
ETL Calibration	0.078	0.237	0.095
ARM Calibration	0.101	0.219	0.117

Cloud Retrieval Results

To derive the spatial distribution of liquid water clouds we focused on producing CLP retrievals at different angles for the period of CIC IOP. For the reason previously explained, we preferred to apply ARM calibration for such analysis.

Figure 1 shows CLP time series retrieved from C1 radiometer at all scanning angles on April 3, 2003, from 06 Universal Time Coordinates (UTC) to 9.50 UTC. This example shows a cloud coming from the west, which is observed first at 19.35° angle, and then is progressively detected at the other angles. The cloud system is weakening when it is detected by higher angles, revealing that it is moving in a slant direction. To confirm our investigations we considered sky infrared temperature measurements provided by the ARM infrared thermometer (IRT) for the same period (see Figure 2). The IRT is a ground-based radiation pyrometer operating within the spectral range of 9.6 to 11.5 µm where the transmission of the atmosphere is high, thus providing measurements of the equivalent black body brightness temperature emitted by the sky or cloud-base. From the analysis we evaluated the first structure composed of broken clouds or maybe cirrus, while the second front is confirmed to be composed of extended middle clouds. This was also shown when we examined the active remotely-sensed clouds locations (ARSCL) Cloud base heights value-added product (VAP) (http://www.gim.bnl.gov/armclouds/arscl/arscl.html) derived by ceilometer and micropulse lidar (MPL) data.

In Figure 3, we present a second example of cloud retrieval results for the time April 18, 2003. CLP time series from MWR C1 are reported, at elevation angles 19.35° (west direction) and 160.65° (east direction) corresponding to air mass 3, and at elevation angles 30.15° and 149.85° that correspond to air mass 2.5. Liquid analysis at all scanning angles revealed a cloud front coming from the west, passing zenith and moving rapidly to the east. Because the event happened during the day, this behavior was confirmed from the images presented in Figure 4, sampled during the same time period by the ARM Total Sky Imager (TSI), a sky imager system equipped with a hemispherical mirror that is operating at SGP site.
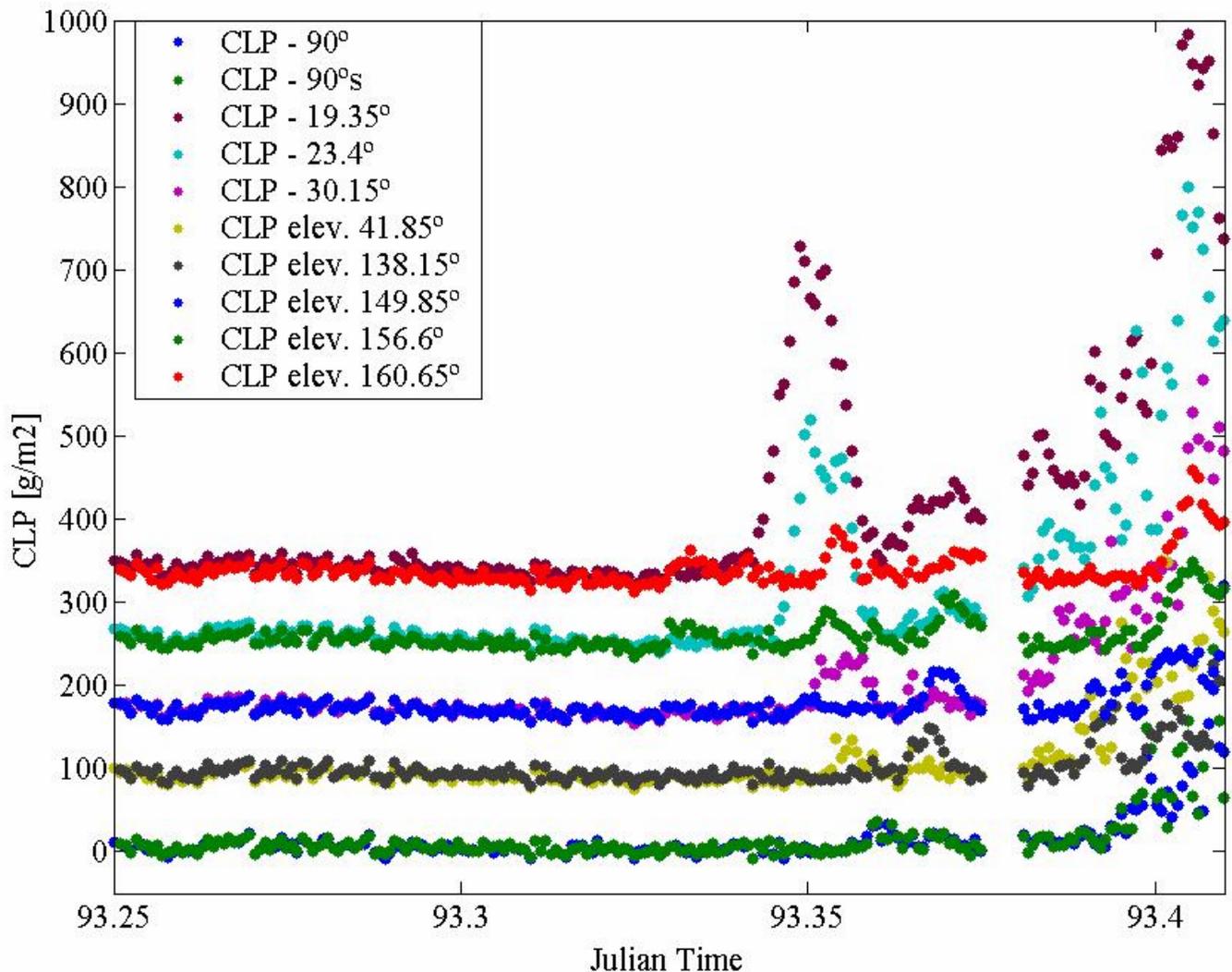
Figure 1. CLP time series from MWR C1 for April 3, 2003, from 6:00 UTC to 9:50 UTC. C1 scans from west to east at angles, 19.35, 23.4, 30.15, 41.85°, 90°, 138.15°, 149.85°, 156.6°, and 90° second scan. An offset has been added to CLP values for clarification of the figure.

Conclusion

MWR has shown its scanning capability to provide information on clouds when measurements are analyzed at different angles. For this reason the operational C1 could provide useful information if it were operated differently from its usual mode, i.e., not going to the LOS mode when clouds appear.
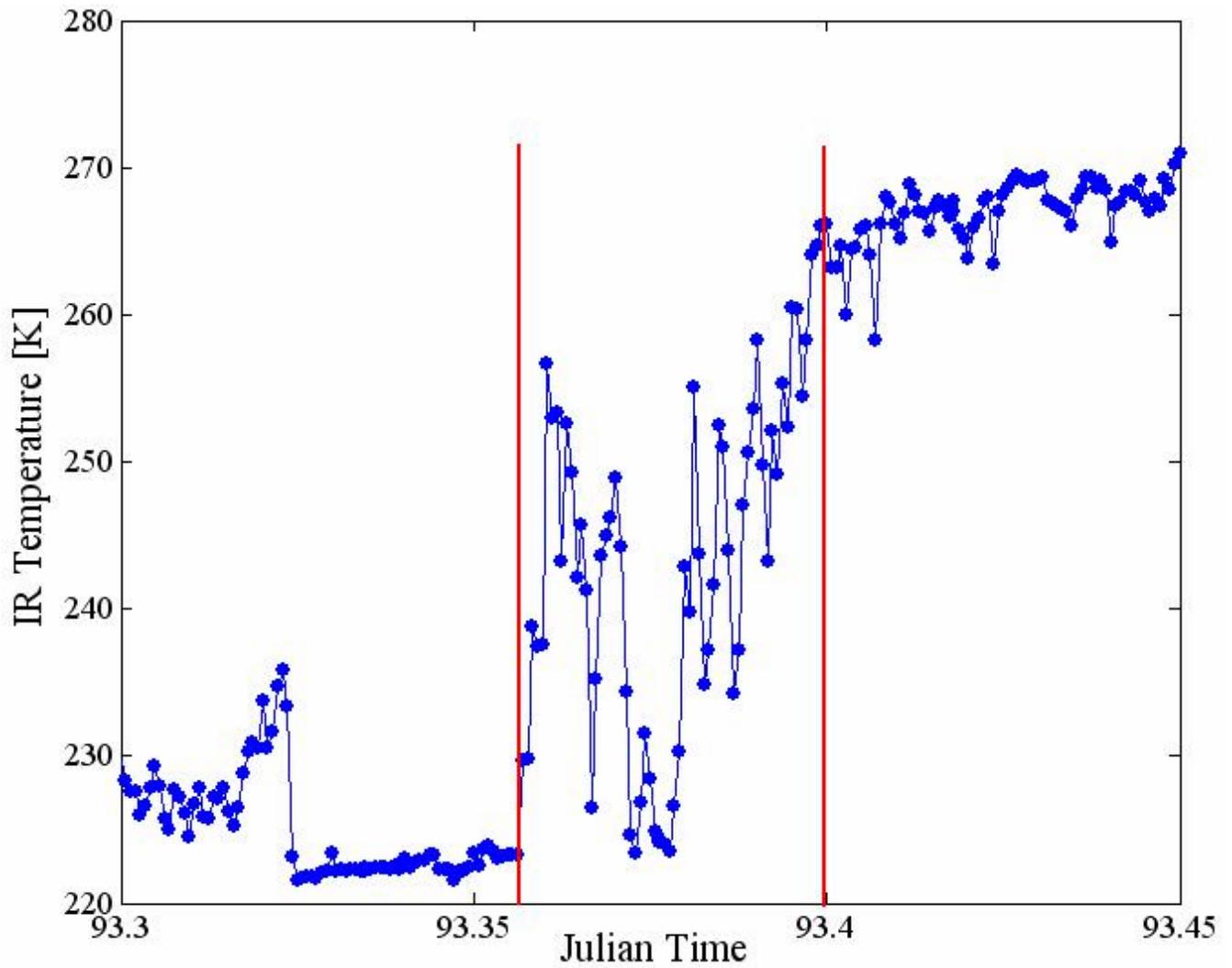
Acknowledgements

Figure 2. IRT sky temperature for April 3, 2003 from 6:00 UTC to 10:50 UTC.
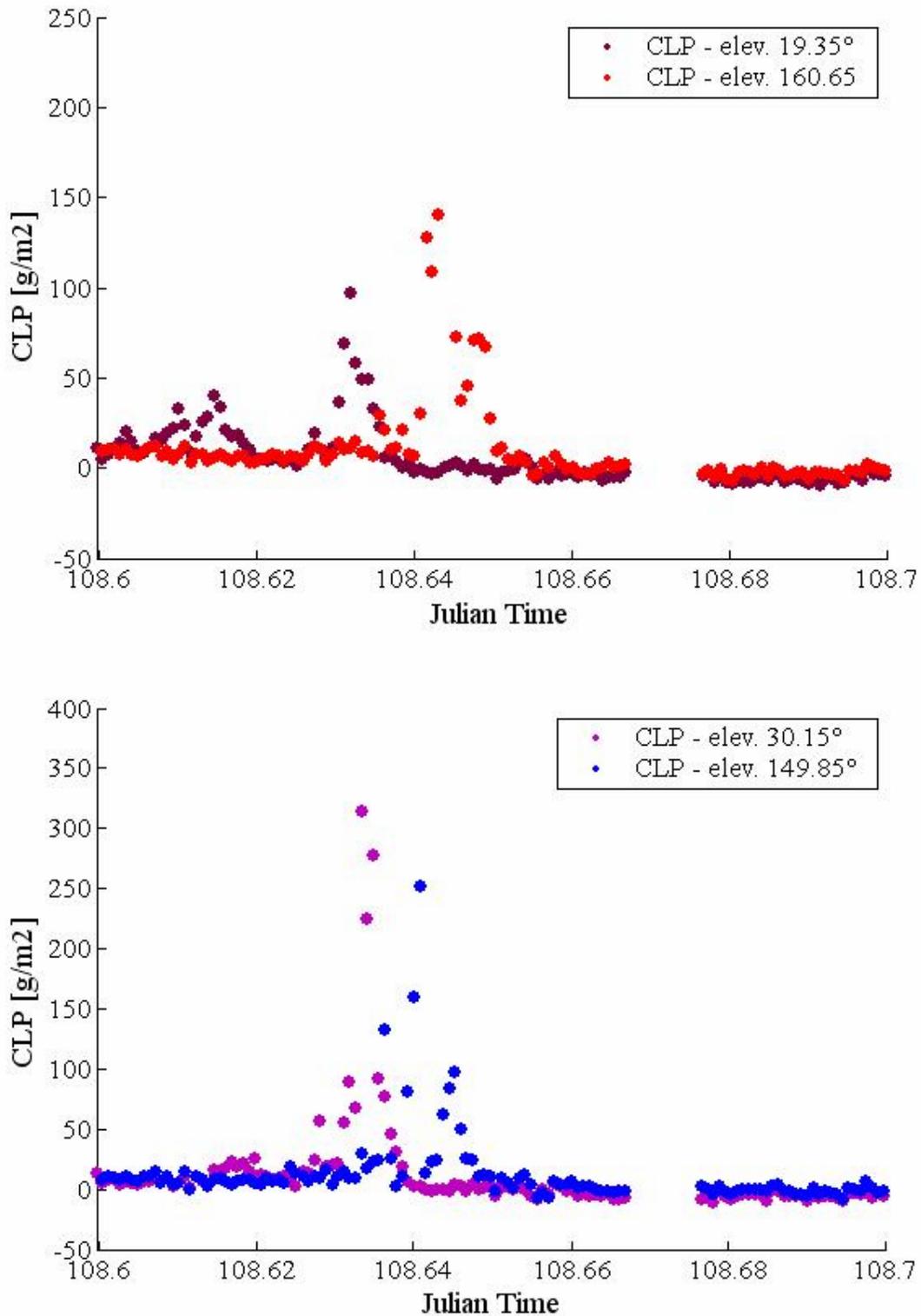
Figure 3. CLP time series for April 18, 2003, derived from MWR C1 at angles 19.35° and 160.65° (upper figure); CLP time series at angles 30.15° and 149.85° (lower figure).

Figure 4. TSI images at SGP site for April 18, 2003. Samples refer to 14:48 UTC, 15:18 UTC and 15:31 UTC, respectively.

Corresponding Author

Vinia Mattioli, mattioli@diei.unipg.it, +39-075-5853660

References

Basili, P., S. Bonafoni, R. Ferrara, P. Ciotti, E. Fionda, and R. Ambrosini, 2001: Atmospheric water vapor retrieval by means of both a GPS network and a microwave radiometer during an experimental campaign at Cagliari (Italy) in 1999. *IEEE Trans. Geosci. Rem. Sen.*, **39**(11), 2436–2443.

Cimini, D., E. R. Westwater, and B. M. Lesht, 2002: Evaluation of recent improvements in humidity sounding by balloon-born sensors. *Proceedings of the COST720 Workshop*, June 19-21, 2002, L'Aquila, Italy. (http://www.aquila.infn.it/people/Nico.Cimini.html/Reprints/ Paper_COST720_RS90_format.pdf)

Cimini, D., E. R. Westwater, Y. Han, and S. Keihm, 2002: Ground-based microwave radiometer measurements and radiosondes comparisons during the WVIOP2000 field experiment. In *Proceedings of the Twelfth Atmospheric Radiation Measurement (ARM) Science Team Meeting*, ARM-CONF-2002. U.S. Department of Energy, Washington, D.C. Available URL: http://www.arm.gov/publications/proceedings/conf12/extended_abs/cimini2-d.pdf

Cimini, D., E. R. Westwater, Y. Han, and S. J. Keihm, 2003: Ground-based microwave radiometer measurements and radiosondes comparisons during the WVIOP2000 field experiment. *Transactions on Geoscience and Remote Sensing,* **41**(11), 2605–2615.

Han, Y., J.B. Snider, E. R. Westwater, S. H. Melfi, and R. A. Ferraro, 1994: Observations of water vapor by ground-based microwave radiometers and Raman lidar. *J. Geophys. Res.*, **99**, 18695–18702.

Han, Y., and E. R. Westwater, 2000: Analysis and improvement of tipping calibration for ground-based microwave radiometers. *IEEE Trans. Geosci. Rem. Sen.,* **38**(3), 1260–1276. http://www.gim.bnl.gov/armclouds/arscl/arscl.html

Liljegren, J. C., 2000: *Automatic self-calibration of ARM microwave radiometers, Microwave Radiometry and Remote Sensing of the Earth's Surface and Atmosphere*, eds., P. Pampaloni and S. Paloscia, pp. 433-443.

Rocken, C., T. van Hove, J. Johnson, F. Solheim, R. Ware, M. Bevis, S. Chiswell, and S. Businger, 1995: GPS/STORM-GPS sensing of atmospheric water vapor for meteorology. *J. Atmos. Oceanic Technol.*, **12**, 468–478.

Rosenkranz, P. W., 1998: Water vapor microwave continuum absorption: A Comparison of Measurements and Models. *Radio Sci.*, **33**, 919–928.

Schroeder, J. A., and E. R. Westwater, 1993: *User's Guide to WPL Microwave Transfer Software*, NOAA Tech Memo ERL WPL-213.

Wang, J., H. L. Cole, D. J. Carlson, E. R. Miller, K. Beirle, A. Paukkunen, and T. K. Laine, 2002: Correction of humidity measurement errors from the Vaisala RS80 radiosonde-Application to TOGA COARE data. *J. Atmos. Oceanic Technol.*, **19**, 981–1002.

Westwater, E. R., 1993: *Ground-based microwave remote sensing of meteorological variables, in Atmospheric Remote Sensing by Microwave Radiometry*, ed., M. A. Janssen, pp. 145-213, John Wiley, New York.

Westwater, E. R., Y. Han, M. D. Shupe, and S. Y. Matrosov, 2001: Analysis of integrated cloud liquid and precipitable water vapor from microwave radiometers during the Surface Heat budget of the Artic Ocean project. *J. Geophys. Res.*, **106**(D23), 32,019–32,030.